Journal of Engineering Research and Applied Science
Available at www.journaleras.com
Volume 15 (1), June 2026, pp 22-30
ISSN 2147-3471 © 2026

Energy and Surface Quality Analysis of AA6063 Alloy During Sulfuric Acid Anodizing at Different Bath Temperatures

Hacer Pınar Vural, Kemal Ermiş*

Mechanical Engineering, Sakarya University of Applied Sciences, Sakarya, Turkey

Accepted 20 May 2026

Abstract
This study investigates the influence of anodizing bath temperature on coating properties, microstructure evolution, and cooling energy demand during sulfuric acid anodizing of AA6063 aluminum alloy. Experimental studies were carried out using 20 wt.% sulfuric acid electrolyte at a constant current density of 15 A/dm² and anodizing duration of 30 minutes. Coating thickness, Vickers microhardness, and scanning electron microscopy (SEM) analyses were performed to evaluate the coating quality. In addition, a thermodynamic cooling load model was developed to estimate the energy consumption of the anodizing bath cooling system. Results indicate that bath temperature significantly affects oxide layer morphology, pore structure, and mechanical properties. It has been observed that the coating thickness increases as the anodizing bath temperature increases. Microhardness values ranged from 459 HV to 534 HV, depending on process temperature. SEM observations revealed homogeneous pore distribution at 19–20°C, while dissolution effects became dominant at 22°C. Energy analysis showed that increasing bath temperature from 18 °C to 20 °C reduces cooling energy demand by approximately 17%. The combined analysis suggests that the optimal operating window for AA6063 sulfuric acid anodizing is between 19 °C and 20°C, providing a balance between coating quality and energy efficiency.

Keywords: *AA6063 alloy, anodizing, energy efficiency, SEM, coating properties*

1. Introduction

Aluminum and its alloys are widely used in engineering applications due to their low density, high strength-to-weight ratio and excellent corrosion resistance. These properties make aluminum alloys particularly attractive for industries such as construction, transportation, aerospace and consumer products. Among various aluminum alloys, AA6063 alloy is one of the most widely used materials in extrusion applications due to its good formability, excellent surface finish and favorable mechanical properties [1]. One of the most widely used surface treatment techniques for aluminum alloys is anodizing. Anodizing is an electrochemical oxidation process in which aluminum is converted into aluminum oxide under the influence of an applied electric field in an electrolyte solution. The anodic oxide layer produced during this process provides improved corrosion resistance, increased surface hardness and enhanced aesthetic properties [2]. The structure of anodic oxide films typically consists of a porous outer layer and a barrier layer near the metal interface. Process parameters such as electrolyte composition, current density, temperature, and anodizing time play critical roles in determining coating properties [3]. Among these parameters, bath temperature has a particularly significant influence on oxide growth kinetics. Temperature affects both oxide formation and dissolution reactions in the electrolyte. Therefore, controlling the bath temperature is essential to obtain coatings with optimal thickness, hardness, and pore morphology.

Furthermore, maintaining low bath temperature requires industrial cooling systems, which leads to significant energy consumption. For this reason, identifying an optimal temperature window that balances coating quality and energy efficiency is an important challenge for anodizing facilities.

Previous studies have extensively investigated the influence of anodizing parameters on aluminum oxide microstructure. Thompson reported that the porous anodic alumina structure strongly depends on electrolyte composition and temperature. Higher temperatures accelerate oxide dissolution, resulting in larger pore diameters and lower coating hardness [4]. Sheasby and Pinner described the industrial anodizing process in detail and highlighted the importance of temperature control in sulfuric acid anodizing.

*Corresponding author: ermis@subu.edu.tr

According to their findings, most industrial anodizing processes operate between 18 °C and 22 °C to maintain stable oxide growth [5].

Other researchers have investigated the microstructural evolution of anodic oxide layers using SEM, EDS and other techniques [6-9]. These studies demonstrated that pore distribution and barrier layer thickness depend strongly on electrochemical parameters. In addition to surface morphology, mechanical properties such as hardness and wear resistance also vary with anodizing conditions.

Energy consumption in anodizing plants has also been studied in the context of industrial sustainability. Cooling systems used to maintain electrolyte temperature represent a significant portion of the total energy demand of anodizing lines. Therefore, optimizing operating temperature not only affects coating quality but also significantly influences operating costs.

Cooling systems used in industrial processes have also been studied extensively in the field of thermal engineering. McQuiston et al. [10] provided a comprehensive analysis of heating, ventilating and air conditioning systems, including heat exchangers and refrigeration cycles commonly used in industrial cooling applications.

Similarly, Perry and Green [11] presented detailed design methodologies for heat exchangers and industrial cooling systems in the widely used chemical engineering handbook. Their work demonstrated that heat transfer efficiency and temperature differences play a crucial role in determining the energy consumption of cooling systems.

Although previous studies have provided valuable insights into anodizing processes and cooling system efficiency, relatively few studies have investigated the combined influence of anodizing parameters and cooling energy consumption. Most research has focused either on coating properties or on thermal system design, but not on the interaction between these two aspects.

Therefore, there is a clear need for studies that integrate surface engineering analysis with energy efficiency evaluation. Such an integrated approach can provide valuable guidance for optimizing industrial anodizing processes in terms of both coating performance and energy consumption.

This study investigates the influence of bath temperature on coating properties and cooling energy consumption during sulfuric acid anodizing of AA6063 aluminum alloy. This article presents an energy-analysis–dominant evaluation of anodizing bath temperature for AA6063 in sulfuric acid.

The present study aims to investigate the influence of bath temperature on the anodizing behavior of AA6063 aluminum alloy and to evaluate its effect on cooling energy consumption using a simplified heat-transfer model. By combining microstructural characterization with energy analysis, the study aims to identify the optimal temperature range for industrial anodizing operations. The study combines experimental characterization (thickness, hardness, SEM) with a detailed mathematical model of cooling load and refrigeration performance to identify an operating window that balances coating quality and cooling electricity.

2. Materials and Methods

2.1. Material

Heat-treated AA6063 (T5) extruded profiles were used as the substrate material. The alloy is an Al–Mg–Si system commonly selected for extrusion applications.

2.2. Anodizing Procedure

The anodizing process involves the electrochemical oxidation of aluminum in an acidic electrolyte solution under the influence of direct current [5]. In this process, the aluminum workpiece acts as the anode while a suitable cathode material completes the electrical circuit. When electrical current passes through the electrolyte, oxidation reactions occur at the aluminum surface and a controlled oxide layer forms.

The anodic oxide layer is primarily composed of aluminum oxide (Al_2O_3). The oxide film grows simultaneously at the metal–oxide interface and dissolves at the oxide–electrolyte interface. The balance between these two mechanisms determines the final thickness and morphology of the anodic layer [3].

Surface preparation is a critical step in anodizing operations. Typical pretreatment steps include degreasing, alkaline etching and acid neutralization to ensure uniform oxide growth during the anodizing stage. Figure 1 shows the anodizing flowchart.

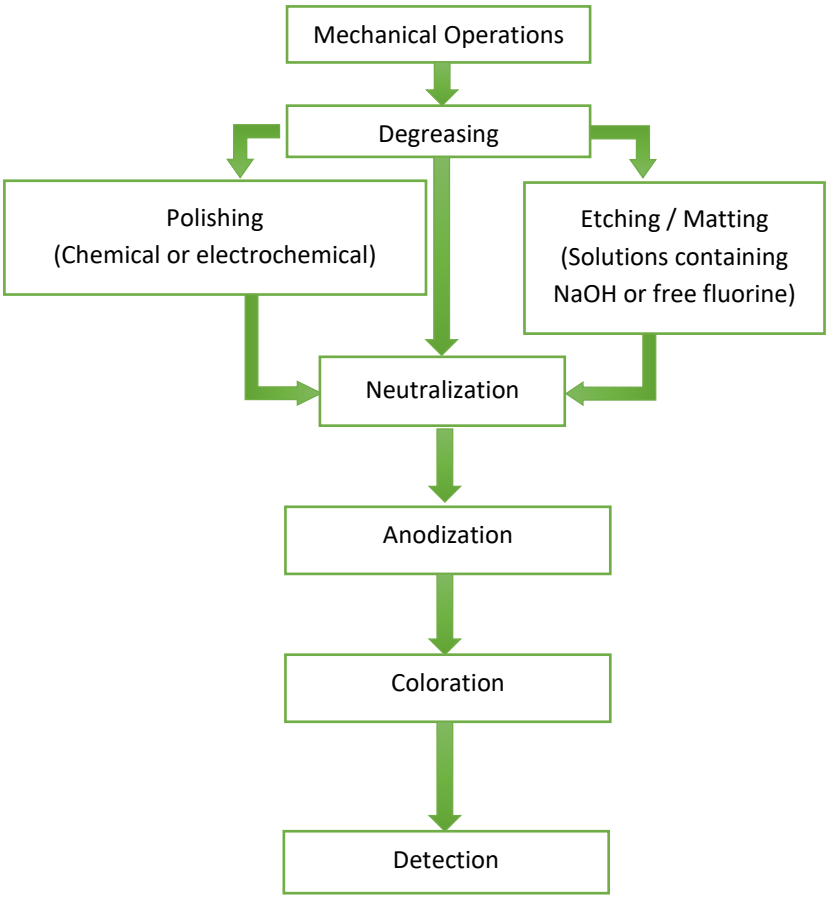

Figure 1. Anodizing flowchart.

- Degreasing process: Degreasing is applied to remove processing oils, press oil, human-generated oil, and dust residues from the profile surface. Baths containing 2–5% alkaline or neutral detergent are generally preferred at a temperature of 50–70 °C. The degreasing time ranges from 3 to 10 minutes, depending on the bath concentration and the part's level of contamination. This step is quite important in terms of preventing coating defects [12].
- Alkaline Matt Bath (Etching) process: After degreasing, alkaline matt baths are used to remove naturally formed oxide layers on the profile surface and to mattify the surface. These baths consist of a 5–15% NaOH (sodium hydroxide) solution. The process temperature is 50–70 °C, and the duration is generally 2–5 minutes. In this step, microscopic irregularities on the surface are increased, facilitating the adhesion of the anodizing layer [5].
- Acidic Matt Bath process: Acidic matt baths are used as an alternative or complement to alkaline matt baths, particularly in applications where a more homogeneous matt finish and decorative appearance are desired on the surface. These baths often contain sulfuric acid and small amounts of fluoride compounds. The process takes 2–5 minutes, and the temperature is maintained between 30–50 °C [5].
- Neutralization (Desmutting) process: Acidic neutralization baths are applied to neutralize insoluble iron or other metal oxides remaining on the surface after alkaline or acidic matting. A 25–30% sulfuric acid solution is usually preferred. The neutralization process takes 1–3 minutes. This process is critically important in preventing color defects and peeling in anodized coatings [5, 12].

During anodizing, the reaction occurs as follows:
Anode reaction (formation of aluminum oxide layer):

$$2Al + 3H_2O \rightarrow Al_2O_3 + 6H^+ + 6e^- \quad (1)$$

Cathode reaction (hydrogen gas is released):

$$6H^+ + 6e^- \rightarrow 3H_2 \quad (2)$$

Net Reaction:

$$2Al + 3H_2O \rightarrow Al_2O_3 + 3H_2 \quad (3)$$

In this process, the anode is the positive pole to which the aluminum profiles are connected in the anodizing bath. It is the source of electrons and the electrode where the oxidation reaction takes place. The cathode is the negative pole, usually made of lead, aluminum, or stainless steel, which is immersed in the bath. It receives electrons during the reaction and completes the circuit. Figure 2 shows a visual representation of

the anodizing process and the resulting chemical reaction.

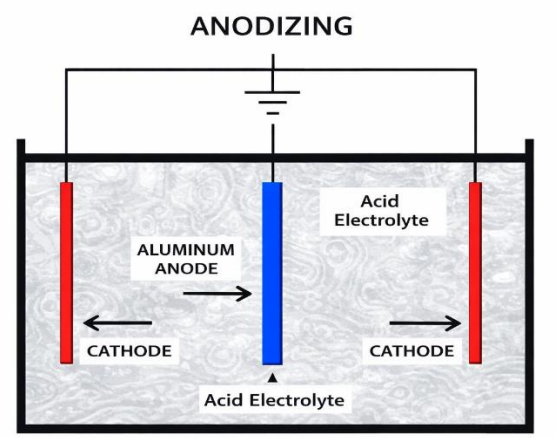

Figure 2. Visual representation of the anodizing process.

Table 1. Anodizing conditions for the experimental study

Parameter	Value
Electrolyte	20 wt.% H_2SO_4
Current density (J)	15 A/dm²
Time (τ)	30 min
Bath temperature	18, 19, 20, 21, 22 °C

The desired surface quality can be achieved by optimizing parameters such as electrolyte temperature and current density in these chemical reactions. Increasing the temperature increases the dissolution rate of the oxide layer, leading to a decrease in quality, while low temperatures can reduce process efficiency.

Experimental studies were carried out using an electrolyte containing 20 wt.% sulfuric acid at a constant current density of 15 A/dm² for 30 minutes. Five bath temperatures were investigated: 18 °C, 19 °C, 20 °C, 21 °C and 22 °C. Pre-treatment steps (degreasing, etching/matting, neutralization) were implemented as described in the thesis to ensure surface cleanliness and consistent oxide growth. Table 1 shows the anodizing conditions for the anodizing coating on AA 6063 alloy in the experimental procedures. Coating thickness measurements were performed using optical microscopy. Microhardness measurements were performed using the Vickers indentation technique. Surface morphology and cross-sectional microstructure were examined using scanning electron microscopy (SEM).

3. Energy and Heat-Transfer Modeling Framework

The success of the anodizing process largely depends on controlling the process temperature. Figure 3 shows a schematic representation of the cooling unit [13].

The temperature in the coating bath has a critical effect on the growth rate, quality, and mechanical properties of the oxide layer [1, 9]. Therefore, a suitable cooling system is necessary to maintain a stable and optimum temperature.

Figure 4 schematically summarizes the thermal management architecture used in anodizing lines.

In this architecture, heat from the anodizing bath is sent from the acid circulation pump to the heat exchanger unit. The bath heat is extracted from the heat exchanger and sent to an industrial chiller or chiller-cooling tower to be removed before being sent back to the anodizing bath.

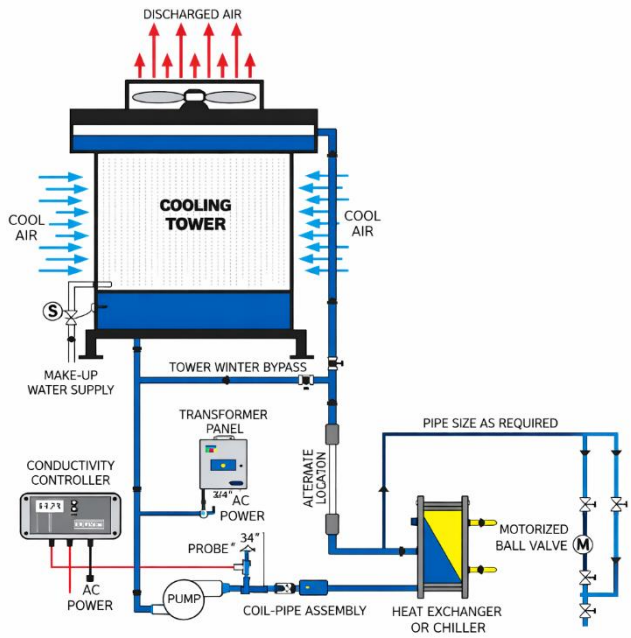

Figure 3. Schematic representation of the cooling unit.

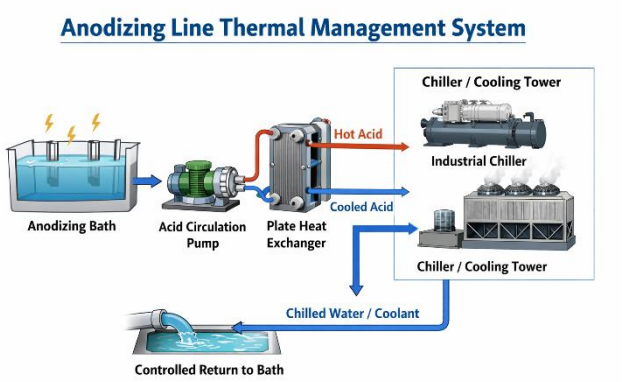

Figure 4. The thermal management architecture used in anodizing lines.

3.1. Electrical Input, Heat Generation, and Bath Heat Balance

During anodizing, the rectifier supplies direct current to drive electrochemical oxidation. The electrical power input is:

$$P_{el} = V \text{ x } I \quad (4)$$

where V is the cell voltage and I is the total current.

If the anodized surface area is A_s (dm²) and the current density is J (A/dm²), then $I = J \times A_s$. The electrical energy delivered over time τ is:

$$E_{el} = P_{el} \text{ x } \tau \quad (5)$$

A fraction of this electrical energy contributes to oxide formation and reaction enthalpies, while the remainder appears as heat in the electrolyte and surrounding system. For an engineering cooling-load estimate consistent with the thesis approach, the dominant thermal term is taken as the net heat that must be removed to maintain a steady bath temperature setpoint:

$$Q_{cool} \approx Q_{gen} - Q_{loss} \quad (6)$$

where $\dot{Q}_{gen}$ is the process heat generation rate and $\dot{Q}_{loss}$ aggregates passive losses to ambient via tank walls, evaporation, and carryover. Under stable operating conditions, the required cooling duty equals the net heat input to the bath.

3.2. Cooling Load from Fluid Energy Balance

The cooling duty transferred through the bath-to-exchanger circuit can be computed from the circulating electrolyte mass flow rate:

$$\dot{Q} = \dot{m}_{bath} \times C_{p,bath} \times (T_{in} - T_{out}) \quad (7)$$

where $\dot{m}_{bath}$ is the electrolyte mass flow rate, $C_{p,bath}$ is the specific heat capacity, and T_{in}/T_{out} are the temperatures at the inlet and outlet of the heat exchanger.

This relation provides a direct link between bath setpoint and required flow/temperature lift. Similarly, on the secondary side (chilled water or glycol loop), the heat absorbed by the refrigerant-side evaporator is:

$$\dot{Q}_{evap} = \dot{m}_{ch} \times C_{p,ch} \times \left(T_{ch,out} - T_{ch,in}\right) \quad (8)$$

3.3. Plate Heat Exchanger Design Using the LMTD Method

For the plate heat exchanger described in the thesis, the transferred duty can also be expressed using the overall heat-transfer coefficient U and heat-transfer area A_{HT}:

$$\dot{Q} = U \times A_{HT} \times LMTD \quad (9)$$

The logarithmic mean temperature difference (LMTD) for counterflow operation is:

$$\text{LMTD} = \frac{\Delta T_1 - \Delta T_2}{\ln\left(\frac{\Delta T_1}{\Delta T_2}\right)} \quad (10)$$

where $\Delta T_1 = (T_{hot,in} - T_{cold,out})$ and $\Delta T_2 = (T_{hot,out} - T_{cold,in})$.

This formulation enables sizing checks: for a target duty $\dot{Q}$ at a given bath setpoint, the required area is:

$$A_{HT} = \frac{\dot{Q}}{U \text{ x LMTD}} \quad (11)$$

3.4. Chiller Performance Metrics: COP and EER

The coefficient of performance (COP) defines refrigeration efficiency:

$$COP = \frac{\dot{Q}_{cool}}{\dot{W}_{in}} \quad (12)$$

where $\dot{W}_{in}$ is the electrical power to the compressor and associated auxiliaries.

The energy efficiency ratio (EER) is commonly used in HVAC practice and relates cooling capacity to electrical input; it can be treated as a scaled variant of COP depending on the unit system.

For annual electricity consumptiothe n estimation, the model uses an operational schedule and computes:

$$E_{year} = \Sigma\left(\dot{W}_{in} \times \Delta t\right) \quad (13)$$

The annual cost is obtained by multiplying by the relevant electricity tariff.

4. Results

4.1. Coating Thickness

In anodizing studies on AA6063 aluminum alloy, coating thickness was measured at two points after anodizing at five bath temperatures between 18 and 22 °C in 1 °C increments [13]. The average of these measurements for each temperature was taken to determine the coating thickness values, and the results are shown in Table 2. The load and dwell time used in the measurements were kept constant, thus ensuring that the effect of temperature could be compared. Coating thickness increases with rising temperature, but dissolution occurs at high temperatures.

Table 2. Coating thickness results

Temperature (°C)	1. Measurement (µm)	2. Measurement (µm)	Average (µm)
18	9.54	9.03	9.29
19	13.48	13.91	13.70
20	12.33	12.76	12.55
21	13.55	12.77	13.16
22	13.98	14.83	14.41

Table 3. Vickers microhardness results according to bath temperature.

Temperature (°C)	Vickers average microhardness (HV)
18	508.3
19	512.7
20	526.0
21	459.0
22	534.0

4.2. Coating Microhardness

In this study, hardness measurements were performed at multiple points on the coating cross-section for each bath temperature; three measurement values were obtained for samples at 18, 19, 20, 21, and 22 °C. The load and holding time used in the measurements were kept constant, thus ensuring the comparability of the effect of temperature [13]. The average Vickers microhardness (HV) values obtained at different bath temperatures are presented in Table 3.

When Table 3 is examined, it is seen that the hardness values are quite close to each other at 18 and 19 °C, and the average hardness is 508.3 and 512.7 HV, respectively. At 20 °C, the average hardness is seen to increase to 526 HV. This indicates that the layer formed at 20 °C is advantageous in terms of both hardness level and homogeneity. At 21 °C, the hardness value decreased to 459 HV; this indicates a significant decrease compared to other temperatures. Although the hardness is higher at 22 °C as 534 HV, the increase in dissolution traces and pore merging in the microstructure suggests that this temperature should be evaluated cautiously in terms of long-term corrosion performance. However, the possibility that the result at this temperature represents a local weak region should not be ignored. Hardness is a function not only of film thickness but also of porosity, pore distribution, and microcrack formation. More compact and highly consistent structures can exhibit higher hardness under micro-indentation. From this perspective, the relatively regular pore structure and good layer continuity of the 20 °C sample in the SEM findings are consistent with the high and reproducible hardness values obtained at this temperature [14]. At low bath temperatures, the dissolution rate of the oxide layer remains limited, and a denser, more compact Al_2O_3 layer is formed. This results in a better microstructure and acceptable Vickers hardness values. In contrast, with increasing temperature, the dissolution mechanism becomes dominant at the electrolyte-oxide interface, leading to pore widening and a decrease in layer density. This structural change causes a decrease in surface hardness.

4.3. SEM Observations

Scanning electron microscopy revealed significant differences in pore morphology depending on bath temperature, as shown in Figure 5 [15]. SEM cross-sections showed that 18–20 °C produced more regular pore morphology and higher layer continuity, whereas at 22 °C dissolution effects increased. Samples anodized at 18 °C exhibited relatively compact oxide layers with fine pore structures. When the temperature increased to 19 °C and 20 °C, the oxide layer became thicker while maintaining structural continuity. This temperature range produced the most uniform pore distribution.

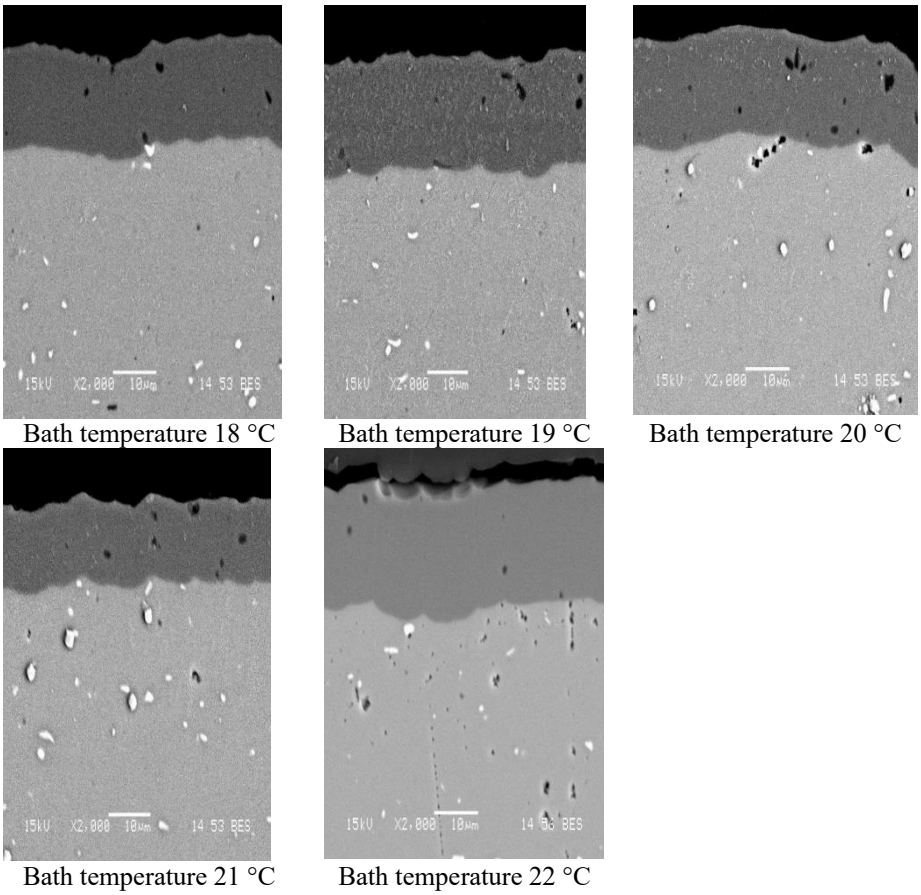

Figure 5. Cross-sectional SEM images of AA6063 aluminum samples anodized at different bath temperatures (2000 x 10 µm magnification)

When the SEM images were examined:
• A more regular pore structure was observed in the 18–20 °C range.
• High-layer continuity.
• Homogeneous surface morphology.
At higher temperatures, such as 21 °C and 22 °C, SEM images showed evidence of partial oxide dissolution.

At 22°C, it was determined that the dissolution effects increased and the structural integrity of the layer was partially disrupted. The pore diameter increased and pore walls became thinner, indicating accelerated chemical dissolution of the oxide layer.

4.4. Energy efficiency analysis

In the energy analysis, the effect of bath temperature on cooling systems was examined. The electrical consumption of the cooling unit was evaluated for an external reference temperature of 30 °C, based on different bath temperatures for anodizing coating. As the temperature of the anodizing bath decreases, the amount of heat that needs to be removed from the system increases. This increases the energy consumption of cooling systems. In this study, it is shown how there will be a difference in the energy consumption of the cooling system if the anodizing coating bath is operated at suitable operating temperatures of 18, 19 and 20 °C, which are appropriate according to the morphological results. The numerical values used are exemplary and should be updated with the facility's own operating data for a real facility.

The assumptions accepted in this study: The characteristic temperature value for the environment where the anodizing line is located is 30 °C and the average electrical power (reference) of the cooling system at 18 °C is 50 kW. The annual operating time of the system is 6000 hours, the electricity unit price is 0.108 USD/kWh and the COP value is considered constant in the range of 18-20 °C.

The annual cooling energy consumption and cost comparison calculated according to the above assumptions is given in Table 4.

Table 4 shows that operating the anodizing bath at 19°C instead of 18°C results in approximately an 8% reduction in the cooling system's electrical energy consumption, while operating it at 20°C results in approximately a 17% reduction.

Table 4. Comparison of annual cooling energy consumption and costs based on the operating temperature of the anodizing bath

	Operating temperature (°C)		
	18	19	20
Relative power, P_{el} (kW)	50	45.8	41.7
Annual energy consumption, E_{year} (kWh/yıl)	300000	275000	250000
Annual cost, $C_{yıl,20}$ (USD/year)	32400	29700	27000
Savings compared to 18 °C (%)	-	8.3	16.7

5. Conclusions

Bath temperature significantly affects coating thickness and microhardness for AA6063 anodized in 20 wt.% H_2SO_4 at 15 A/dm² for 30 min. Coating thickness increases with rising temperature, but dissolution occurs at high temperatures. The Vickers microhardness results obtained in this study show that the anodizing bath temperature has a decisive effect on the surface hardness of AA6063 aluminum profiles. According to the findings, the overall hardness of the anodized layer increases with increasing bath temperature. A significant decrease trend was observed, especially after a certain temperature of 21 °C. This trend is consistent with the basic formation-dissolution mechanisms reported in the literature for sulfuric acid-based anodizing processes. The oxide layer dissolves more slowly at low bath temperatures, resulting in the formation of a denser, more compact Al_2O_3 layer. Better microstructure and acceptable Vickers hardness values are the outcome of this. On the other hand, pore widening and a drop in layer density result from the dissolution mechanism taking over at the electrolyte-oxide interface as the temperature rises. Surface hardness decreases as a result of this structural alteration. In terms of surface hardness, a temperature

range of 18–20 °C was found to be more appropriate for AA6063 aluminum profiles.

SEM analysis revealed that the most uniform oxide morphology occurred within the temperature range of 18–20 °C. The microstructural observations, therefore, support the conclusion that moderate temperatures provide a balance between oxide growth and dissolution, resulting in improved coating quality.

Operating the anodizing bath at 19 °C instead of 18 °C results in approximately an 8% reduction in the cooling system's electrical energy consumption, while operating it at 20 °C results in approximately a 17% reduction in electrical energy consumption.

The optimum anodizing bath temperature range for AA6063 is approximately 19–20 °C, considering both coating quality and energy efficiency.

References

[1]. Guo, F., Cao, Y., Wang, K., Zhang, P., Cui, Y., Hu, Z., & Xie, Z. (2022). Effect of the anodizing temperature on microstructure and tribological properties of 6061 aluminum alloy anodic oxide films. Coatings, 12(3), 314.

[2]. Białek, E., Włodarski, M., & Norek, M. (2020). Influence of anodization temperature on geometrical and optical properties of porous anodic alumina (PAA)-based photonic structures. Materials, 13(4), 3185.

[3]. Hatch, J. (1984). Aluminum: Properties and physical metallurgy. ASM International.

[4]. Thompson, G. (1997). Porous anodic alumina: Fabrication, characterization and applications. Thin Solid Films, 297(1-2), 192-201.

[5]. Sheasby, P. G., & Pinner, R. (2001). The surface treatment and finishing of aluminium and its alloys (6th ed.). ASM International.

[6]. Goldstein, J. I. (2018). Scanning electron microscopy and X-ray microanalysis (4th ed.). Springer.

[7]. Lee, W., & Park, S. J. (2014). Porous anodic aluminum oxide: Anodization and templated synthesis of functional nanostructures. Chemical Reviews, 114(15), 7487-7556.

[8]. O'Sullivan, J. P., & Wood, G. C. (1970). The morphology and mechanism of formation of porous anodic films on aluminium. Proceedings of the Royal Society of London. Series A, Mathematical and Physical Sciences, 317(1531), 511–543.

[9]. Lin, Y. C. (2020). Performance analysis and optimization of industrial anodizing cooling systems. Applied Thermal Engineering, 169, 114968.

[10]. McQuiston, F. C., Parker, J. D., Spitler, J. D., & Taherian, H. (2023). Heating, ventilating, and air conditioning: analysis and design. John Wiley & Sons.

[11]. Perry, R., & Green, D. (2008). Perry's chemical engineers' handbook (8th ed.). McGraw-Hill.

[12]. Davis, J. (2001). Aluminum and aluminum alloys. ASM International.

[13]. Chiller.com.tr. (2024). Hava soğutmalı chiller modelleri. Chiller: https://www.chiller.com.tr/hava-sogutmali-chiller/hava-sogutmali-chiller-modelleri.

[14]. Vural H. P., Ermiş, K. (2026). 6063 Alüminyum Profillerde Eloksal Kaplama Sıcaklığının Yüzey Sertliğine Etkileri, 4th International Conference on Pioneer and Innovative Studies ICPIS 2026, Konya / Turkey, ISBN: 978-625-8676-28-0.

[15] Vural H. P., Ermiş, K. (2026). Sülfürik Asit Eloksal Prosesinde Banyo Sıcaklığının Alüminyum Alaşımının Yüzey Özelliklerine Etkisi, 7. Bölüm, Mühendislikte Trend ve Yenilikçi Araştırmalar, Editör: Umut Özkaya, All Sciences Academy yayınları, ISBN: 978-625-8676-58-7, Sayfa:115-134.